Title	Soluble Klotho causes hypomineralization in Klotho-deficient mice
Auther(s)	Minamizaki, Tomoko; Konishi, Yukiko; Sakurai, Kaoru; Yoshioka, Hirotaka; Aubin, Jane E.; Kozai, Katsuyuki; Yoshiko, Yuji
Citation	Journal of Endocrinology , 237 (3) : 285 - 300
Issue Date	2018-06
DOI	10.1530/JOE-17-0683
Self DOI	
URL	http://ir.lib.hiroshima-u.ac.jp/00049037
Right	This document is the Accepted Manuscript version of a Published Work that appeared in final form in Journal of Endocrinology, copyright © Society for Endocrinology after peer review and technical editing by the publisher. To access the final edited and published work see https://doi.org/10.1530/JOE-17-0683. This is not the published version. Please cite only the published version. この論文は出版社版でありません。引用の際には出版社版をご確認、ご利用ください。
Relation	

Soluble Klotho causes hypomineralization in Klotho-deficient mice

Tomoko Minamizaki,[1]* Yukiko Konishi,[1,2]* Kaoru Sakurai,[1,2] Hirotaka Yoshioka,[1] Jane E. Aubin,[3] Katsuyuki Kozai,[2] Yuji Yoshiko[1]

[1] Department of Calcified Tissue Biology, School of Dentistry, Hiroshima University Graduate School of Biomedical & Health Sciences, 1-2-3, Kasumi, Minami-ku, Hiroshima 734-8553, Japan

[2] Department of Pediatric Dentistry, School of Dentistry, Hiroshima University Graduate School of Biomedical & Health Sciences, 1-2-3, Kasumi, Minami-ku, Hiroshima 734-8553, Japan

[3] Department of Molecular Genetics, University of Toronto, 1 King's College Circle, Toronto, Ontario M5S 1A8, Canada

*Tomoko Minamizaki and Yukiko Konishi contributed equally to this work.

Corresponding author

Yuji Yoshiko, Ph.D.

Department of Calcified Tissue Biology, School of Dentistry, Hiroshima University Graduate School of Biomedical & Health Sciences, 1-2-3, Kasumi, Minami-ku, Hiroshima 734-8553, Japan

Tel.: +81 82 257 5620

Fax: +81 82 257 5621

E-mail: yyuji@hiroshima-u.ac.jp

Running headline: sKL causes hypomineralization in *kl/kl* mice

Abstract

The type I transmembrane protein αKlotho (Klotho) serves as a coreceptor for the phosphaturic hormone fibroblast growth factor 23 (FGF23) in kidney, while a truncated form of Klotho (soluble Klotho, sKL) is thought to exhibit multiple activities, including acting as a hormone, but whose mode(s) of action in different organ systems remains to be fully elucidated. FGF23 is expressed primarily in osteoblasts/osteocytes and aberrantly high levels in the circulation acting via signaling through an FGF receptor (FGFR)-Klotho coreceptor complex cause renal phosphate wasting and osteomalacia. We assessed the effects of exogenously added sKL on osteoblasts and bone using Klotho-deficient (*kl/kl*) mice and cell and organ cultures. sKL induced FGF23 signaling in bone and exacerbated the hypomineralization without exacerbating the hyperphosphatemia, hypercalcemia and hypervitaminosis D in *kl/kl* mice. The same effects were seen in rodent bone models *in vitro*, in which we also detected formation of a sKL complex with FGF23-FGFR and decreased *Phex* (gene responsible for X-linked hypophosphatemic rickets (XLH)/osteomalacia) expression. Further, sKL-FGF23-dependent hypomineralization *in vitro* was rescued by soluble PHEX. These data suggest that exogenously added sKL directly participates in FGF23 signaling in bone and that PHEX is a downstream effector of the sKL-FGF23-FGFR axis in bone.

Introduction

αKlotho (Klotho) is a type I transmembrane protein with a large extracellular domain, a single-pass membrane-spanning segment, and a short intracellular carboxyl terminus without any phosphorylation sites. Klotho hypomorphic (*kl/kl*) mice display various anomalies resembling a human senescence-related phenotype, including skin and muscle atrophy, vascular calcification, and premature death (Kuro-O *et al*. 1997). In humans, a homozygous missense mutation (H193R) in KLOTHO is involved in severe tumoral calcinosis with dural and carotid artery calcifications (Ichikawa *et al*. 2007). *KLOTHO* gene polymorphisms (G395A in the promoter region and C1818T in exon 4) have also been associated with bone mineral density and multiple pathophysiologies in humans (Kawano *et al*. 2002, Shimoyama *et al*. 2009).

Klotho is highly expressed in kidneys and forms a complex with and converts canonical fibroblast growth factor receptors (FGFRs), in particular FGFR1, into a specific receptor for fibroblast growth factor 23 (FGF23), a phosphaturic hormone (ADHR Consortium 2000, Kurosu *et al*. 2006, Urakawa *et al*. 2006). It is therefore perhaps not surprising that loss of function of Klotho shares many common features with loss of function of FGF23 in mice, including increased serum levels of phosphate (Yoshida *et al*. 2002, Shimada *et al*. 2004b). FGF23, secreted primarily by osteoblasts and osteocytes (Riminucci *et al*. 2003, Yoshiko *et al*. 2007b), circulates in blood and acts together with membrane Klotho in renal tubules to suppress phosphate reabsorption and vitamin D_3 activation (Shimada *et al*. 2004a, Shimada *et al*. 2004b, Larsson *et al*. 2004). Consistent with this, *kl/kl* mice have extremely high levels of serum FGF23, and exhibit hyperphosphatemia, hypervitaminosis D, and hypophosphatemic disorders (Segawa *et al*. 2007).

The widespread effects of Klotho deficiency on tissues/organs not expressing Klotho, such as seen in *kl/kl* mice and conditions of Klotho haploinsufficiency in humans have suggested that Klotho functions through a circulating and, as yet, undefined, hormonal factor(s) (Kuro-O *et al*. 1997, Kawaguchi *et al*. 1999, Kawano *et al*. 2002, Shimoyama *et al*. 2009). Three Klotho protein types have been identified: a full-length transmembrane Klotho, a truncated soluble Klotho (sKL), and a secreted Klotho (Kuro-O *et al*. 1997, Matsumura *et al*. 1998, Wang & Sun 2009, Xu & Sun 2015). All types have been detected in humans and mice, but only the transmembrane and soluble Klotho proteins have been detected in rats (Wang & Sun 2009, Matsumura *et al*. 1998). sKL, arising from cleavage (shedding) of membrane Klotho by the metalloproteinase (ADAM) family members ADAM10 and ADAM17 (Chen *et al*. 2007) and a secreted Klotho by alternative splicing of *Klotho* are thought to be released into the circulation (Matsumura *et al*. 1998, Wang & Sun 2009, Xu & Sun 2015), but the function of sKL and secreted Klotho is not clear. Exact concentrations of serum sKL also remain uncertain, in part due to different forms of sKL and secreted Klotho and differences measured with different immunoassays, but levels of less than a few hundred nanograms per milliliter are seen in mice and humans (Kurosu *et al.* 2005, Pedersen *et al*. 2013). Treatment with sKL or transgenic overexpression of sKL extends mouse lifespan with multiple effects on insulin/insulin-like growth factor-I, TGF-ß and Wnt signaling (Kurosu *et al.* 2005, Liu *et al.* 2007, Chen *et al*. 2013), interaction with vascular endothelial growth factor receptor (VEGF)-2 and endothelial transient-receptor potential canonical Ca^{2+} channels to regulate Ca^{2+} influx in aorta (Kusaba *et al*. 2010), and hydrolyzation of the glycosylated transient receptor potential ion channel TRPV5 in kidney (Chang *et al*. 2005, Wolf *et al*. 2014).

Previously, we demonstrated hypomineralization in osteoblast cultures overexpressing FGF23 (Wang *et al*. 2008). sKL has also been shown to interact with FGF23 (Kawai *et al*. 2013) and decrease chondrocyte proliferation via FGFR3 but increase proliferation while inhibiting differentiation-mineralization via FGFR1 in the MC3T3-E1 osteoblastic cell model (Shalhoub *et al*. 2011, Kawai *et al*. 2013). To further assess whether sKL contributes to FGF23 actions in bone, and to eliminate confounding effects of membrane-associated Klotho, we used *kl/kl* mice supplemented with and without sKL. We found that sKL promotes FGF23 signaling in *kl/kl* bone and downregulates *Phex*, which contributes, at least in part, to sKL-FGF23-induced inhibition of bone mineralization.

Materials and Methods

Animals

Klotho mutant mice (*kl*/+; CREA Japan, Tokyo, Japan), C57BL/6J mice, and timed-pregnant Wistar rats (Charles River Laboratories Japan, Yokohama, Japan) use and procedures were approved by the Institutional Animal Care and Use Committee at Hiroshima University (Approval #A09-36). Genotyping of *kl/kl* mice and wild type (WT) littermates was performed as described previously (Brownstein *et al*. 2010).

Male C57BL/6J mice (age, 4 wk) were treated with 1α,25-dihydroxyvitamin D3 (1,25 D; 6 μg/kg in ethanol:polyethylene glycol at 1:4 [vol/vol]; Enzo Life Sciences, Farmingdale, NY) subcutaneously once per day for 2 d, followed 24 h later by a single intravenous injection of sKL (10 μg/kg in PBS) or vehicle (PBS) alone (Hines *et al*. 2004; Kawai *et al*. 2013). Sera, kidneys, and bones were harvested 2 h after the sKL injection. Male *kl/kl* and age-matched

WT mice were treated with a subcutaneous sKL (or vehicle) injection (10 µg/kg; R&D Systems, Minneapolis, MN) in 0.5% atelocollagen as carrier in PBS (Koken, Tokyo, Japan) into the dorsum every second day from postnatal day 10 (P10) to P22 (group *kl/kl* + sKL). Calcein (10 mg/kg in 2% sodium bicarbonate) was injected intraperitoneally twice, at P14 and P20. All samples were collected at P22.

Cell and organ cultures

The reagents used (final concentrations given in parentheses) were: 1,25D (1–10 nM); FGF23 and sKL (500 ng/ml each, unless otherwise specified; R&D Systems); MAPK inhibitors (for ERK, U0126; for JNK, dicumarol; and for p38MAPK, SB203580; 10 µM each). All other chemicals, unless otherwise specified, were purchased from Sigma-Aldrich (St. Louis, MO). These reagents were dissolved as appropriate in ethanol, PBS, or DMSO, and maintained at −20 or −80°C until use. Heparin (1 µg/ml) was included along with FGF23 when cells were maintained under serum-deprived conditions (see below).

We isolated calvarial cells from 21-d-old fetal rats or newborn *kl/kl* and WT mice as described previously (Wang *et al*. 2008; Minamizaki *et al*, 2009). Cells were cultured in α-MEM containing 10% fetal bovine serum (FBS; HyClone; GE Healthcare Life Sciences, Logan, UT) and 50 µg/ml ascorbic acid (osteogenic medium). Unless otherwise stated, cells adapted to serum-deprived conditions (0.1% FBS in αMEM) for 24 h were used for mineralization studies; to induce matrix mineralization, cells were treated with 2 mM ß-glycerophosphate for the last 24 h of culture and stained for ALP/von Kossa, followed by quantification using imageJ (Bellows *et al*. 1986). We have previously reported the temporal

expression profiles of osteoblast markers during differentiation and mineralization in rat calvarial (RC) cell cultures (Minamizaki *et al*. 2009).

RC cells transfected with human FGF23 recombinant adenoviruses (Adv-hFGF23) or adenoviruses expressing β-galactosidase (Adv-βgal; BD Biosciences, San Jose, CA) were obtained as described elsewhere (Wang *et al*. 2008).

For organ culture, two fragments (approximately 1.5 × 3 mm) randomly selected from parietal bones of WT or *kl/kl* mice were placed on a cell culture insert in a well (BD Biosciences) in BGJb medium supplemented with 0.1% bovine serum albumin and recombinant human BMP-2 (50 ng/ml; PeproTech, Rocky Hill, NJ) for 24 h, followed by fresh medium with or without sKL.

FGF23, 1,25D, phosphate, and calcium concentrations

We measured FGF23 concentrations in sera, conditioned media, and/or lysates of kidneys and bones by using an FGF23 ELISA kit (intact FGF23, Kainos, Tokyo, Japan). Serum 1,25D and phosphate/calcium concentrations were quantified using a radioimmunoassay (TFB, Tokyo, Japan) and calorimetric determination kits (Wako Pure Chemical, Osaka, Japan), respectively. Protein concentrations were determined using the BCA protein assay (Thermo Fisher Scientific, Waltham, MA).

Western blotting

Lysates or eluates from immunomagnetic separation were subjected to SDS-PAGE and blotted onto polyvinylidene difluoride membranes, which were incubated with primary antibodies (polyclonal antibodies against FGF23, phosphorylated and non-phosphorylated

ERK1/2; 1:1000; Santa Cruz) and then HRP-conjugated secondary antibodies (1:2000; Santa Cruz).

Reverse transcription and PCR analysis

Total RNA was extracted using TRIzol reagent (Invitrogen, Carlsbad, CA), reverse transcribed (ReverTra Ace®; Toyobo, Osaka, Japan) and subjected to quantitative real-time PCR (StepOnePlus; Life Technologies, Carlsbad, CA) as described (Yoshiko *et al*. 2007a, Faul *et al.* 2011). ß-actin (*in vivo*) or ribosomal protein L32 (*in vitro*) was used as internal control. Primer and amplicon information is in Table 1.

Histological and morphological assays

Tissues were fixed in 4% paraformaldehyde in PBS and plastic sections prepared according to the manufacturer's instructions. Bone mineralization was evaluated using calcein double-labeling (Choi *et al*. 2017). Plastic sections were also carbon-coated and elemental mapping of magnesium, calcium, and phosphorus was performed using electron probe microanalysis with a beam current of 20 nA and an accelerating voltage of 15 kV with an integration time of 0.05 s at each pixel (JXA-8200; JEOL, Tokyo, Japan) (Suzuki *et al*. 2008). The RGB (red, green, blue) color intensity was quantified by ImageJ. Decalcified paraffin sections (10% EDTA in PBS) were used for hematoxylin and eosin or immunofluorescence staining. Frontal sections (thickness, 5 μm), approximately 2-mm from the sagittal suture, were used for histomorphometry. Sections pretreated with Dako® protein block (Dako, Glostrup, Denmark) were incubated with a mixture of polyclonal antibodies against FGF23 and pERK1/2 or with polyclonal antibodies against PHEX (1:60; Santa Cruz Biotechnology, Dallas, TX) at 4°C

overnight, followed by incubation with a mixture of Cy2- and/or Cy3-conjugated (1:400; Jackson ImmunoResearch Laboratories, West Grove, PA) or Alexa Fluor® 594 (1:500; ThermoFisher Scientific, Waltham, MA)-conjugated secondary antibodies for 1 h at room temperature. FGF23- and pERK-positive areas on the sections were quantified by ImageJ.

Immunoprecipitation

Cell lysates, prepared in 1% IGEPAL CA630 and 50 mM Tris HCl (pH 8.0), were incubated with protein G-conjugated magnetic microbeads (Miltenyi Biotec Inc., San Diego, CA) plus mouse monoclonal antibody against FGFR1 or control IgG for 30 min on ice under rotary agitation, followed by rinsing and elution to obtain immune complexes in accordance with the manufacturer's recommendations.

DNA microarray

Total RNA (1 μg; evaluated by RIN value) was extracted from Adv-hFGF23- or Adv-βgal-transfected RC cells (n=3 replicates for each) and used for generation of second-strand cDNA, and cRNA was amplified with the Oligo dT primer, biotinylated and fragmented with One-Cycle Target Labeling and control reagents (Affymetrix, Santa Clara, CA), followed by hybridization to the GeneChip Rat Genome 230 2.0 Array overnight according to the manufacturer's protocol.

Statistical analysis

Data are presented as mean ± SD (n = 3–4 *in vitro*, n = 5–9 *in vivo*). Experiments were repeated a minimum of two times. Statistical differences were analyzed with one-way

ANOVA using *post-hoc* Tukey's test for multiple comparisons and *t*-tests for between group comparisons.

Results

sKL is involved in FGF23 signaling in *kl/kl* bones

As expected, serum FGF23 (full length intact FGF23) level was much higher in *kl/kl* compared to WT mice (Fig. 1A, Supplemental Fig. 1A), as were levels of serum calcium (Fig. 1B), phosphate (Fig. 1C) and 1α,25-dihydroxyvitamin D_3 (1,25D) (Fig. 1D). *Fgf23* expression (Fig. 1E) and accumulation (Fig. 1F) in bone and kidney was also higher in *kl/kl* compared to WT mice. Notably, administration of sKL to *kl/kl* mice increased ERK1/2 phosphorylation (pERK1/2) in bone but not kidney (Fig. 1G), and did not change serum parameters tested. As for the renal FGF23 target genes, *Cyp27b1* levels were higher in *kl/kl* than in WT mice (Fig. 1H), while *Slc34a1* (Fig. 1I) and *Slc34a3* (Fig. 1J) were equally expressed among all groups. Neither the Klotho deficiency in *kl/kl* mice nor sKL supplementation had any significant effect on the levels of *Galnt 3* mRNA whose product (*N*-acetylgalactosaminyltransferase 3) *O*-glycosylates FGF23 to prevent proteolytic processing by the subtilisin-like proprotein convertase FURIN in bone and kidney (Fig. 1K) (Kato *et al*. 2006, Frishberg *et al*. 2007, Tagliabracci *et al*. 2014). *Furin* mRNA levels (Fig. 1L) was significantly higher in kidney but not bone of *kl/kl* mice. sKL had no effect on the reduced weight gain exhibited by *kl/kl* compared to WT mice (Supplemental Fig. 1B). Short term treatment of WT mice with sKL had no effect on serum parameters, gene expression in kidney or bone, or bone parameters (see below; data not shown).

sKL potentiates ERK signaling in bones of normal Klotho-expressing mice treated with 1,25D

To determine whether sKL elicits similar responses to those seen in *kl/kl* mice in normal Klotho-expressing mice treated with 1,25D, we treated C57BL/6J mice with 1,25D followed by a single injection of sKL. As expected (Kolek *et al*. 2005, Yamamoto et al. 2010), 1,25D increased not only *Fgf23* expression (Fig. 2A) and accumulation (Fig. 2B) in bone, but also increased levels of serum FGF23 (Fig. 2C) and calcium (Fig. 2D). 1,25D treatment had no effect on serum phosphate levels (Fig. 2E), but decreased levels of the FGF23 target genes in kidney (see above) (Fig. 2F-H) and increased pERK1/2 in bone and kidney (Fig. 2I and J). Notably, the 1,25D-induced increase in pERK1/2 in bone was further enhanced by sKL treatment within 2 h (Fig 2I and J). Thus, exogenously added sKL activates the ERK pathway in not only *kl/kl* but also normal bone.

sKL causes mineralization defects in *kl/kl* bones

Given that sKL activated ERK1/2 in bone of *kl/kl* mice, we hypothesized that sKL might improve the skeletal anomalies seen in *kl/kl* mice. However, electron probe X-ray microanalysis of parietal bones revealed lower calcium and phosphorus, and higher magnesium signals in bones of sKL-treated *kl/kl* mice versus in WT or vehicle-treated *kl/kl* mice (Fig. 3A and Suppl. Fig. 2). Reduced calcein double-labeling (Fig. 3B) and increased osteoid thickness (Fig. 3C and D) paralleled the electron probe X-ray microanalysis data. sKL treatment had no detectable effect on osteoblast number (Fig. 3E), osteocyte number (Fig. 3F) or bone thickness (Fig.3G). Osteoblasts and osteocytes were markedly FGF23-positive in *kl/kl* but not WT bone, with intense FGF23-pERK co-expression in bone of sKL-treated mice (Fig. 4A). Concomitantly, the expression of the osteoblast/osteocyte marker genes (Fig. 4B-G) with the exception of *Bglap* (Fig. 4D) tended to be higher in *kl/kl*

compared to WT bone, with *Spp1* (Fig. 4B), *Dmp1* (Fig. 4E), *Mepe* (Fig. 4G) and *Phex* (Fig. 4H) significantly higher; of these, only *Phex* was decreased significantly by sKL treatment. No significant changes were detectable in *Fgfr1* mRNA expression under any condition.

sKL directly promotes FGF23 signaling and hypomineralization of bone *in vitro*

To determine whether sKL directly regulates FGF23-dependent signaling in bone, we assessed *kl/kl* and WT mouse calvaria cells in osteogenic medium *in vitro*. *kl/kl* calvaria cells exhibited intrinsic anomalies with fewer ALP-positive (ALP^+) cells (Fig. 5A) and lower matrix mineralization (Fig. 5B) than their WT counterparts. FGF23 was very low to undetectable in both WT and *kl/kl* cells (Fig. 5C), with undetectable expression of *Klotho* but elevated levels of *Fgf23* mRNA in bones (Fig. 5D). These results suggest that the intrinsic defects in *kl/kl* osteoblasts are independent of FGF23 levels. Consistent with this possibility, although FGF23 production was high in *kl/kl* up to at least 48 h in calvaria organ cultures (Fig. 5E), expression of early growth response-1 (*Egr-1*), another marker of FGF23 signaling (Kurosu *et al*. 2006) (Fig. 5F), and pERK1/2 (Fig. 5G) was increased in *kl/kl* calvaria organ cultures only on treatment with sKL. Similarly, *Egr-1* expression (Fig. 5H) and ERK1/2 activation (Fig. 5I) were seen in the rat calvaria (RC) cell osteogenic model only when sKL was used in combination with FGF23. These results indicate that sKL directly promotes FGF23 signaling in bones.

Phex is a downstream effector of sKL-FGF23-FGFR signaling in osteoblasts

To identify the gene(s) acting downstream of sKL-FGF23-FGFR signaling in osteoblasts-osteocytes, we used the RC cell model during mineralization phase of culture (Minamizaki *et*

al. 2009). We first confirmed that endogenous FGF23 coprecipitated FGFR1 in the presence of sKL in RC cells pretreated with 1,25D (Fig. 5J). Second, we confirmed that matrix mineralization is defective in RC cells when they are treated with sKL plus FGF23 (Fig. 6A). Of more than 31,000 genes screened by microarray analysis, 52 genes were differentially expressed in sKL-FGF23-treated versus untreated RC cells; of these, 16 genes were downregulated (Table 2). Of these sixteen genes, only *Phex* has previously been implicated in bone mineralization, with Phex haploinsufficiency causing osteomalacia/X-linked hypophosphatemic rickets in mice and humans (Guo & Quarles 1997, Miao et al. 2001). qRT-PCR confirmed that sKL downregulated *Phex* in both RC cell culture (Fig. 6B) and *kl/kl* bone organ culture (Fig. 6C) models. As expected based on its activity to stimulate FGF23 (Kolek *et al*. 2005, Yamamoto et al. 2010), 1,25D also downregulated *Phex* in the RC cell model (Fig. 6D). Treatment of RC cells with soluble PHEX (sPHEX) in the presence of sKL and FGF23 rescued the hypomineralization caused by sKL and FGF23 (Fig. 6E). Finally, the sKL-FGF23-induced hypomineralization of RC cell cultures was also rescued by U0126, an inhibitor of ERK activation involved FGF23 signaling, but not the c-Jun N-terminal kinase (JNK) inhibitor dicumarol or the p38 MAP kinase inhibitor SB203580 (Fig. 6F). Taken together, our findings suggest that sKL-FGF23 induces ERK1/2 activation in bone leading to downregulation of *Phex* and hypomineralization.

Discussion

Much remains to be understood about the relationship between sKL, the Klotho-FGF23 axis and mineralization of bone. In this study, we assessed the effects of exogenously added sKL on bone and osteoblasts using Klotho-deficient (*kl/kl*) mice and cell and organ cultures. We found that sKL induced FGF23 signaling and ERK1/2 activation in bone and exacerbated the *kl/kl* hypomineralization defect without exacerbating the hyperphosphatemia, hypercalcemia or hypervitaminosis D seen in these mice. We also report that sKL formed a complex with FGF23 and FGFR, caused ERK1/2-dependent downregulation of *Phex* and that the sKL-FGF23-dependent hypomineralization was rescued by treatment with soluble PHEX *in vitro*. These data suggest that exogenously added sKL participates directly in FGF23 signaling in bone and that PHEX is a downstream effector of the sKL-FGF23-FGFR axis in bone (Fig. 7).

Interactions among the type I membrane protein Klotho, FGF23, and FGFR1 suggest that the target cells of FGF23 express Klotho, as seen in kidney (Kurosu *et al*. 2006, Urakawa *et al*. 2006, Ben-Dov *et al*. 2007, Lindberg *et al*. 2014). Klotho expressed in osteocytes has been reported to play a key role in bone mineralization (Komaba *et al*, 2017), in spite of 500 times lower Klotho in bone than kidney (Rhee *et al*. 2011) and undetectable Klotho expression in osteoblasts (see Fig. 5). Such reports highlight the need to better understand the potential mechanisms by which FGF23 regulates bone mineralization. Consistent with several studies (Goetz *et al*. 2010, Shalhoub *et al*. 2011, Smith *et al*. 2012, Kawai M *et al*. 2013), we found that sKL participates in FGF23-dependent signaling, and in particular we report that sKL negatively regulates bone mineralization both in normal bone cell models and in the complete absence of Klotho in *kl/kl* mice. Taken together, the data raise questions about how

extensively sKL contributes to FGF23-dependent signaling in bones under normal and pathological conditions. The finding that *Fgf23* expression in bones is dependent on the circadian clock system (Kawai *et al*. 2014) further highlights the need for additional studies.

Although sKL forms a complex with FGF23 and FGFRs and subsequently promotes FGF23 signaling in a variety of cells, including NIH3T3 cells treated with increasing concentrations of FGF23 and sKL (Smith et al., 2012) and human embryonic kidney 293 cells overexpressing FGF23 and sKL (Kawai *et al*. 2013), our relatively short-term treatment protocols with sKL inhibited bone mineralization without affecting renal FGF23 target genes or changing serum calcium and phosphate levels in the models used here. Similarly, short-term treatment with sKL did not rescue serum phosphate levels or affect expression of renal FGF23 target genes in neonatal *Hyp* mice, a mouse model of XLH (Kawai *et al*. 2013) nor did sKL enhance the effect of FGF23 treatment alone in kidney slices *ex vivo* (Andrukhova *et al*, 2017). Longer-term administration (intraperitoneally) of sKL has also been shown to rescue ectopic calcification without changes in serum calcium and phosphate levels in *kl/kl* mice (Chen *et al*. 2013); whether short-term administration of sKL also has an inhibitory effect on ectopic mineralization in *kl/kl* mice seems plausible but remains to be determined. Indeed, chronic sKL overexpression driven by a liver-specific promoter in mice resulted in osteomalacia, although this was accompanied by hypophosphatemia, hypocalcemia and markedly increased FGF23, making it difficult to separate sKL effects in kidneys versus bones (Smith *et al*, 2012). Taken together, these results suggest that sKL may not support the actions of FGF23 in kidney, at least under pathologic conditions such as when Klotho or PHEX are deficient, or when FGF23 is overexpressed. In *Hyp* mice, an excess of osteocytic

FGF23 contributes to pyrophosphate accumulation and the resultant mineralization defect through the downregulation of tissue nonspecific ALP (Murali *et al*. 2016). In our models, the elevated levels of *Furin* mRNA in kidney may degrade FGF23, yielding more than a 100-fold difference in FGF23 levels between bone and kidney. The abundant FGF23 in bone may thus provide a suitable environment for complex formation of sKL, FGF23 and FGFRs.

Andrukhova and colleagues reported that FGF23 modulates PTH function via ERK1/2 phosphorylation in bone and kidney (Andrukhova *et al*. 2016). The fact that sKL plus FGF23 treatment upregulates ERK1/2 and *Egr-1* in bone and osteoblastic cells is in keeping with the observation that they are involved in FGF23 signaling in kidneys, parathyroid and chondrogenic cells (Urakawa *et al*. 2006, Ben-Dov *et al*. 2007, Kawai M *et al*. 2013). However, results reported for ERK involvement in bone matrix mineralization have been somewhat contradictory, with ERK sometimes reported as a negative regulator and sometimes a positive regulator of matrix mineralization, likely due to the difficulty of completely separating the effects of ERK on osteoblast differentiation versus matrix mineralization in some models and protocols. For example, studies with transgenic mice overexpressing either a dominant negative *Mek1* or constitutively active *Mek1* driven by the osteocalcin promoter crossed with Runx2$^{+/-}$ mice suggested that ERK–MAPK activation stimulates osteoblast differentiation and skeletal development through a pathway involving RUNX2 (Ge *et al*. 2007). On the other hand, when Kono *et al*. used approaches of chemical inhibition and infection with adenovirus vector-mediated dominant negative Ras or constitutively active Mek1 in MC3T3-E1 cells, MLO-A5 pre-osteocytic cells and over the calvaria of neonatal mice, they concluded that ERK is a negative regulator of matrix

mineralization (Kono *et al*. 2007). Our results on calvaria cells specifically during the mineralization phase of cultures are in keeping with these latter results, and with the view that ERK activation acts as a negative regulator of bone matrix mineralization. That ERK may have apparently opposite effects at different stages of osteogenesis is consistent with a model in which the temporal rate and concentration of growth factors are captured by the Ras and Rap1 systems and encoded into transient or sustained ERK activation, respectively, to deliver distinct biological outcomes (Sasagawa *et al*. 2005). Additional studies to understand the dynamics of ERK activation in different stages of osteogenesis are warranted (see also below).

The notion that ERK signaling has different effects at different stages of osteogenesis is paralleled by results with conditional inactivation of FGFR1 in osteogenic cells or in bones of transgenic mice that suggest a dual role for FGFR1 signaling at different stages of osteoblast maturation (Jacob *et al*. 2006). In osteo-chondroprogenitors or immature osteoblasts, FGFR1 deficiency increased proliferation and delayed differentiation and matrix mineralization, whereas in differentiated osteoblasts, FGFR1 deficiency enhanced mineralization. On the other hand, FGF2 was reported to induce apoptosis in murine differentiating calvaria osteoblasts and in the calvaria suture of mice overexpressing FGF2 through FGFR2 (Mansukhani *et al*. 2000). FGF2 also promoted proliferation in bone marrow stromal cells but inhibited alkaline phosphatase expression and matrix mineralization in mature osteoblasts via FGF23/FGFR/MAPK signaling (Xiao *et al*. 2013). Our data on sKL/FGF23-dependent ERK activation shows that activation is transient, which may explain why FGF23 but not FGF2 acts on mineralization rather than osteogenic cell proliferation and apoptosis (Mansukhani *et*

al. 2000, Shalhoub *et al*. 2011, Xiao *et al*. 2013). It is also worth noting that PDZ-binding motif (TAZ) protein, the coactivator and repressor of the master transcription factors of osteogenesis (Runx2) and adipogenesis (PPARγ), is negatively regulated by FGF2 via JNK signaling in mouse osteoblast MC3T3-E1 cells (Eda *et al*. 2008), while sKL/FGF23-dependent hypomineralization requires the ERK pathway (Kyono *et al*. 2012). *Fgf23* but not *Fgf2* expression is markedly upregulated by 1,25D in osteoblasts/osteocytes, in parallel with the expression of the vitamin D receptor (Yamamoto *et al*. 2010). Taken together with the dynamics of FGFRs during osteoblastogenesis (Wang *et al*. 2008, Su *et al*. 2014), specific cellular settings may provide the specific context in which sKL and FGF23 act on bone mineralization.

The expression of *Phex*, encoding a protein with homology to zinc metallopeptidases on the X chromosome, is mostly limited to osteoblasts/osteocytes and odontoblasts (Ruchon *et al*. 2000). Loss-of-function mutations in *Phex* cause hypophosphatemia and hypomineralization in bones and teeth, possibly through accumulation of phosphaturic factors (Feng *et al*. 2013). Like *kl/kl* mice, *Hyp* mice show high levels of FGF23 (Nakatani *et al*. 2009). Little information is available on Klotho in XLH. Disruption of *Klotho* in *Hyp* mice (Klotho null-*Hyp*) indicates that Klotho is epistatic to PHEX in biochemical parameters and lifespan (Brownstein *et al*. 2010). Taken together with our data on the dowregulation of *Phex* in bones of *kl/kl* mice treated with sKL, we propose the interdependence of FGF23, Klotho (sKL), and PHEX in skeletal homeostasis. It is possible that sKL treatment of Hyp mice may impact bone mineralization, but detecting such mineralization changes may be difficult, given that the downstream effector of sKL-FGF23, i.e., Phex, is inactive in Hyp mice. Our data may

connect two independent findings, that is, the 1,25D-dependent up- and downregulation of *Fgf23* and *Phex* expression, respectively (Hines *et al*. 2004, Kolek *et al*. 2005, Barthel *et al*. 2007). On the other hand, sKL treatment does not alter the gene expression levels of *Spp1*, *Dmp1*, and *Mepe* which are higher in *kl/kl* mouse bones compared by those in WT mice. This result indicates that hypomineralization of bones of *kl/kl* mice treated with sKL appears not to be mediated by these genes.

In summary, treatment of *kl/kl* mice with sKL does not rescue their osteopenia, but rather suppresses bone mineralization. sKL participates in FGF23 signaling in bones of *kl/kl* mice, resulting in ERK1/2 activation and repression of PHEX, which is responsible at least in part for the intrinsic mineralization defects seen in *kl/kl* bone (Fig. 7).

Footnotes

The authors declare that they have no conflicts of interest.

Acknowledgements

We thank S. Suzuki, S. Kitabatake, and Y. Shibata for their technical assistance. We thank E. Bonnelye, Laboratoire de Génomique Fonctionelle de Lyon, for the valuable discussions. This work was supported in part by grants from the Ministry of Education, Science, Sports and Culture, Japan (18592001 and 20592139 to Y.Y. and 21791788 to T.M.), and the Canadian Institutes of Health Research (MOP 83704 to J.E.A.).

References

ADHR Consortium 2000 Autosomal dominant hypophosphataemic rickets is associated with mutations in FGF23. *Nat Genet* **26** 345-348.

Andrukhova O, Streicher C, Zeitz U & Erben RG 2016 *Fgf23* and parathyroid hormone signaling interact in kidney and bone. *Mol Cell Endocrinol*. **436** 224-239.

Andrukhova O, Bayer J, Schüler C, Zeitz U, Murali SK, Ada S, Alvarez-Pez JM, Smorodchenko A & Erben RG 2017 Klotho lacks an FGF23-independent role in mineral homeostasis. *J Bone Miner Res.* **32** 2049-2061.

Barthel TK, Mathern DR, Whitfield GK, Haussler CA, Hopper HA 4th, Hsieh JC, Slater SA, Hsieh G, Kaczmarska M & Jurutka PW 2007 1,25-Dihydroxyvitamin D_3/VDR-mediated induction of FGF23 as well as transcriptional control of other bone anabolic and catabolic genes that orchestrate the regulation of phosphate and calcium mineral metabolism. *J Steroid Biochem Mol Biol* **103** 381-388.

Bellows CG, Sodek J, Yao KL & Aubin JE 1986 Phenotypic differences in subclones and long-term cultures of clonally derived rat bone cell lines. *J Cell Biochem* **31** 153-169.

Ben-Dov IZ, Galitzer H, Lavi-Moshayoff V, Goetz R, Kuro-O M, Mohammadi M, Sirkis R, Naveh-Many T & Silver J 2007 The parathyroid is a target organ for FGF23 in rats. *J Clin Invest* **117** 4003-4008.

Brownstein CA, Zhang J, Stillman A, Ellis B, Troiano N, Adams DJ, Gundberg CM, Lifton RP & Carpenter TO 2010 Increased bone volume and correction of HYP mouse hypophosphatemia in the Klotho/HYP mouse. *Endocrinology* **151** 492-501.

Chang Q, Hoefs S, van der Kemp AW, Topala CN, Bindels RJ & Hoenderop JG 2005 The β-glucuronidase klotho hydrolyzes and activates the TRPV5 channel. *Science* **310** 490-493.

Chen CD, Podvin S, Gillespie E, Leeman SE & Abraham CR 2007 Insulin stimulates the cleavage and release of the extracellular domain of Klotho by ADAM10 and ADAM17. *Proc Natl Acad Sci U S A* **104** 19796-19801.

Chen TH, Kuro-O M, Chen CH, Sue YM, Chen YC, Wu HH & Cheng CY 2013 The secreted Klotho protein restores phosphate retention and suppresses accelerated aging in Klotho mutant mice. *Eur J Pharmacol* **698** 67-73.

Eda H, Aoki K, Marumo K, Fujii K & Ohkawa K 2008 FGF-2 signaling induces downregulation of TAZ protein in osteoblastic MC3T3-E1 cells. Biochem Biophys Res Commun. **366** 471-475.

Faul C, Amaral AP, Oskouei B, Hu MC, Sloan A, Isakova T, Gutiérrez OM, Aguillon-Prada R, Lincoln J & Hare JM *et al.* 2011 FGF23 induces left ventricular hypertrophy. *J Clin Invest* **121** 4393-4408.

Feng JQ, Clinkenbeard EL, Yuan B, White KE & Drezner MK 2013 Osteocyte regulation of phosphate homeostasis and bone mineralization underlies the pathophysiology of the heritable disorders of rickets and osteomalacia. *Bone* **54** 213-221.

Frishberg Y, Ito N, Rinat C, Yamazaki Y, Feinstein S, Urakawa I, Navon-Elkan P, Becker-Cohen R, Yamashita T & Araya K *et al*. 2007 Hyperostosis-hyperphosphatemia syndrome: a congenital disorder of O-glycosylation associated with augmented processing of fibroblast growth factor 23. *J Bone Miner Res* **22** 235-242.

Ge C, Xiao G, Jiang D & Franceschi RT 2007 Critical role of the extracellular signal-regulated kinase-MAPK pathway in osteoblast differentiation and skeletal development. *J Cell Biol* **176** 709-718.

Goetz R, Nakada Y, Hu MC, Kurosu H, Wang L, Nakatani T, Shi M, Eliseenkova AV, Razzaque MS & Moe OW *et al*. 2010 Isolated C-terminal tail of FGF23 alleviates hypophosphatemia by inhibiting FGF23-FGFR-Klotho complex formation. *Proc Natl Acad Sci U S A* **107** 407-412.

Guo R & Quarles LD 1997 Cloning and sequencing of human PEX from a bone cDNA library: evidence for its developmental stage-specific regulation in osteoblasts. *J Bone Miner Res.* **12**1009-1017.

Hines ER, Kolek OI, Jones MD, Serey SH, Sirjani NB, Kiela PR, Jurutka PW, Haussler MR, Collins JF & Ghishan FK 2004 1,25-dihydroxyvitamin D_3 down-regulation of *PHEX* gene expression is mediated by apparent repression of a 110 kDa transfactor that binds to a polyadenine element in the promoter. *J Biol Chem* **279** 46406-46414.

Ichikawa S, Imel EA, Kreiter ML, Yu X, Mackenzie DS, Sorenson AH, Goetz R, Mohammadi M, White KE & Econs MJ 2007 A homozygous missense mutation in human KLOTHO causes severe tumoral calcinosis. *J Clin Invest* **117** 2684-2691.

Jacob AL, Smith C, Partanen J & Ornitz DM 2006 Fibroblast growth factor receptor 1 signaling in the osteo-chondrogenic cell lineage regulates sequential steps of osteoblast maturation. *Dev Biol*. **296** 315-328.

Kato K, Jeanneau C, Tarp MA, Benet-Pagès A, Lorenz-Depiereux B, Bennett EP, Mandel U, Strom TM & Clausen H 2006 Polypeptide GalNAc-transferase T3 and familial tumoral calcinosis. Secretion of fibroblast growth factor 23 requires O-glycosylation. *J Biol Chem* **281** 18370-18377.

Kawaguchi H, Manabe N, Miyaura C, Chikuda H, Nakamura K & Kuro-O M 1999 Independent impairment of osteoblast and osteoclast differentiation in *klotho* mouse exhibiting low-turnover osteopenia. *J Clin Invest* **1104** 229-237.

Kawai M, Kinoshita S, Kimoto A, Hasegawa Y, Miyagawa K, Yamazaki M, Ohata Y, Ozono K & Michigami T 2013 FGF23 suppresses chondrocyte proliferation in the presence of soluble α-Klotho both in vitro and in vivo. *J Biol Chem* **288** 2414-2427.

Kawai M, Kinoshita S, Shimba S, Ozono K & Michigami T 2014 Sympathetic activation induces skeletal *Fgf23* expression in a circadian rhythm-dependent manner. *J Biol Chem* **289** 1457-1466.

Kawano K, Ogata N, Chiano M, Molloy H, Kleyn P, Spector TD, Uchida M, Hosoi T, Suzuki T & Orimo H *et al*. 2002 Klotho gene polymorphisms associated with bone density of aged postmenopausal women. *J Bone Miner Res* **17** 1744-1751.

Kolek OI, Hines ER, Jones MD, LeSueur LK, Lipko MA, Kiela PR, Collins JF, Haussler MR & Ghishan FK 2005 1α,25-Dihydroxyvitamin D_3 upregulates FGF23 gene expression in bone: the final link in a renal-gastrointestinal-skeletal axis that controls phosphate transport. *Am J Physiol Gastrointest Liver Physiol* **289** G1036-1042.

Komaba H, Kaludjerovic J, Hu DZ, Nagano K, Amano K, Ide N, Sato T, Densmore MJ, Hanai JI & Olauson H *et al*. 2017 Klotho expression in osteocytes regulates bone metabolism and controls bone formation *Kidney Int* **92** 599-611.

Kono SJ, Oshima Y, Hoshi K, Bonewald LF, Oda H, Nakamura K, Kawaguchi H, & Tanaka S 2007 Erk pathways negatively regulate matrix mineralization. *Bone* **40** 68-74.

Kuro-O M, Matsumura Y, Aizawa H, Kawaguchi H, Suga T, Utsugi T, Ohyama Y, Kurabayashi M, Kaname T & Kume E *et al*. 1997 Mutation of the mouse *klotho* gene leads to a syndrome resembling ageing. *Nature* **390** 45-51.

Kurosu H, Yamamoto M, Clark JD, Pastor JV, Nandi A, Gurnani P, McGuinness OP, Chikuda H, Yamaguchi M & Kawaguchi H *et al.* 2005 Suppression of aging in mice by the hormone Klotho. *Science* **309** 1829-1833.

Kurosu H, Ogawa Y, Miyoshi M, Yamamoto M, Nandi A, Rosenblatt KP, Baum MG, Schiavi S, Hu MC & Moe OW *et al*. 2006 Regulation of fibroblast growth factor-23 signaling by klotho. *J Biol Chem* **281** 6120-6123.

Kusaba T, Okigaki M, Matui A, Murakami M, Ishikawa K, Kimura T, Sonomura K, Adachi Y, Shibuya M & Shirayama T *et al*. 2010 Klotho is associated with VEGF receptor-2 and the transient receptor potential canonical-1 Ca^{2+} channel to maintain endothelial integrity. *Proc Natl Acad Sci U S A* **107** 19308-19313.

Kyono A, Avishai N, Ouyang Z, Landreth GE, & Murakami S 2012 FGF and ERK signaling coordinately regulate mineralization-related genes and play essential roles in osteocyte differentiation. *J Bone Miner Metab*. **30** 19-30.

Larsson T, Marsell R, Schipani E, Ohlsson C, Ljunggren O, Tenenhouse HS, Jüppner H, & Jonsson KB 2004 Transgenic mice expressing fibroblast growth factor 23 under the control of the α1(I) collagen promoter exhibit growth retardation, osteomalacia, and disturbed phosphate homeostasis. *Endocrinology* **145** 3087-3094.

Lindberg K, Amin R, Moe OW, Hu MC, Erben RG, Östman Wernerson A, Lanske B, Olauson H & Larsson TE 2014 The kidney is the principal organ mediating klotho effects. *J Am Soc Nephrol* **25** 2169-2175.

Liu H, Fergusson MM, Castilho RM, Liu J, Cao L, Chen J, Malide D, Rovira II, Schimel D & Kuo CJ *et al.* 2007 Augmented Wnt signaling in a mammalian model of accelerated aging. *Science* **317** 803-806.

Mansukhani A, Bellosta P, Sahni M & Basilico C 2000 Signaling by fibroblast growth factors (*Fgf*) and fibroblast growth factor receptor 2 (*Fgfr2*)-activating mutations blocks mineralization and induces apoptosis in osteoblasts. *J Cell Biol* **149** 1297-1308.

Matsumura Y, Aizawa H, Shiraki-Iida T, Nagai R, Kuro-O M & Nabeshima Y 1998 Identification of the human klotho gene and its two transcripts encoding membrane and secreted klotho protein. *Biochem Biophys Res Commun.* **242** 626–630.

Miao D, Bai X, Panda D, McKee M, Karaplis A & Goltzman D 2001 Osteomalacia in hyp mice is associated with abnormal phex expression and with altered bone matrix protein expression and deposition. *Endocrinology* **142** 926-939.

Minamizaki T, Yoshiko Y, Kozai K, Aubin JE & Maeda N 2009 EP2 and EP4 receptors differentially mediate MAPK pathways underlying anabolic actions of prostaglandin E_2 on bone formation in rat calvaria cell cultures. *Bone* **44** 1177-1185.

Murali SK, Andrukhova O, Clinkenbeard EL, White KE & Erben RG 2016 Excessive osteocytic *Fgf23* secretion contributes to pyrophosphate accumulation and mineralization xefect in Hyp mice. *PLoS Biol* **14** e1002427.

Nakatani T, Ohnishi M & Razzaque MS 2009 Inactivation of klotho function induces hyperphosphatemia even in presence of high serum fibroblast growth factor 23 levels in a genetically engineered hypophosphatemic (*Hyp*) mouse model. *FASEB J* **23** 3702-3711.

Pedersen L, Pedersen SM, Brasen CL & Rasmussen LM 2013 Soluble serum Klotho levels in healthy subjects. Comparison of two different immunoassays. *Clin Biochem* **46** 1079-1083.

Rhee Y, Bivi N, Farrow E, Lezcano V, Plotkin LI, White KE & Bellido T 2011 Parathyroid hormone receptor signaling in osteocytes increases the expression of fibroblast growth factor-23 *in vitro* and *in vivo*. *Bone* **49** 636-643.

Riminucci M, Collins MT, Fedarko NS, Cherman N, Corsi A, White KE, Waguespack S, Gupta A, Hannon T & Econs MJ *et al*. 2003 FGF-23 in fibrous dysplasia of bone and its relationship to renal phosphate wasting. *J Clin Invest* **112** 683-692.

Ruchon AF, Tenenhouse HS, Marcinkiewicz M, Siegfried G, Aubin JE, DesGroseillers L, Crine P & Boileau G 2000 Developmental expression and tissue distribution of Phex protein: effect of the Hyp mutation and relationship to bone markers. *J Bone Miner Res.* **15** 1440-1450.

Sasagawa S, Ozaki Y, Fujita K & Kuroda S 2005 Prediction and validation of the distinct dynamics of transient and sustained ERK activation. *Nat Cell Biol* **7** 365-373.

Segawa H, Yamanaka S, Ohno Y, Onitsuka A, Shiozawa K, Aranami F, Furutani J, Tomoe Y, Ito M & Kuwahata M *et al*. 2007 Correlation between hyperphosphatemia and type II Na-P_i cotransporter activity in klotho mice. *Am J Physiol Renal Physiol* **292** F769-779.

Shalhoub V, Ward SC, Sun B, Stevens J, Renshaw L, Hawkins N & Richards WG 2011 Fibroblast growth factor 23 (FGF23) and α-klotho stimulate osteoblastic MC3T3.E1 cell proliferation and inhibit mineralization. *Calcif Tissue Int* **89** 140-150.

Shimada T, Hasegawa H, Yamazaki Y, Muto T, Hino R, Takeuchi Y, Fujita T, Nakahara K, Fukumoto S & Yamashita T 2004a FGF-23 is a potent regulator of vitamin D metabolism and phosphate homeostasis. *J Bone Miner Res* **19** 429-435.

Shimada T, Kakitani M, Yamazaki Y, Hasegawa H, Takeuchi Y, Fujita T, Fukumoto S, Tomizuka K & Yamashita T 2004b Targeted ablation of *Fgf23* demonstrates an essential physiological role of FGF23 in phosphate and vitamin D metabolism. *J Clin Invest* **113** 561-568.

Shimoyama Y, Nishio K, Hamajima N & Niwa T 2009 KLOTHO gene polymorphisms G-395A and C1818T are associated with lipid and glucose metabolism, bone mineral density and systolic blood pressure in Japanese healthy subjects. *Clin Chim Acta* **406** 134-138.

Smith RC, O'Bryan LM, Farrow EG, Summers LJ, Clinkenbeard EL, Roberts JL, Cass TA, Saha J, Broderick C & Ma YL et al. 2012 Circulating αKlotho influences phosphate handling by controlling FGF23 production. *J Clin Invest.* **122** 4710-4715.

Su N, Jin M & Chen L 2014 Role of FGF/FGFR signaling in skeletal development and homeostasis: learning from mouse models. *Bone Res*. **2** 14003.

Suzuki H, Amizuka N, Oda K, Noda M, Ohshima H & Maeda T 2008 Histological and elemental analysis of impaired bone mineralization in klotho-deficient mice. *J Anat* **212** 275-285.

Tagliabracci VS, Engel JL, Wiley SE, Xiao J, Gonzalez DJ, Nidumanda Appaiah H, Koller A, Nizet V & White KE et al. 2014 Dynamic regulation of FGF23 by Fam20C

phosphorylation, GalNAc-T3 glycosylation, and furin proteolysis. *Proc Natl Acad Sci U S A* **111** 5520-5525.

Urakawa I, Yamazaki Y, Shimada T, Iijima K, Hasegawa H, Okawa K, Fujita T, Fukumoto S & Yamashita T 2006 Klotho converts canonical FGF receptor into a specific receptor for FGF23. *Nature* **444** 770-774.

Wang H, Yoshiko Y, Yamamoto R, Minamizaki T, Kozai K, Tanne K, Aubin JE & Maeda N 2008 Overexpression of fibroblast growth factor 23 suppresses osteoblast differentiation and matrix mineralization in vitro. *J Bone Miner Res* **23** 939-948.

Wang Y & Sun Z 2009 Current understanding of klotho. *Ageing Res Rev.* **8** 43–51.

Wolf MT, An SW, Nie M, Bal MS & Huang CL 2014 Klotho up-regulates renal calcium channel transient receptor potential vanilloid 5 (TRPV5) by intra- and extracellular N-glycosylation-dependent mechanisms. *J Biol Chem* **289** 35849-35857.

Xiao L, Esliger A & Hurley MM 2013 Nuclear fibroblast growth factor 2 (FGF2) isoforms inhibit bone marrow stromal cell mineralization through FGF23/FGFR/MAPK *in vitro*. *J Bone Miner Res*. **28** 35-45.

Xu Y & Sun Z 2015 Molecular basis of klotho: from gene to function in aging. Endocr Rev **36** 174-193.

Yamamoto R, Minamizaki T, Yoshiko Y, Yoshioka H, Tanne K, Aubin JE, & Maeda N 2010 1α,25-dihydroxyvitamin D_3 acts predominately in mature osteoblasts under conditions of high extracellular phosphate to increase fibroblast growth factor 23 production *in vitro*. *J Endocrinol* **206** 279-286.

Yoshida T, Fujimori T & Nabeshima Y 2002 Mediation of unusually high concentrations of 1,25-dihydroxyvitamin D in homozygous klotho mutant mice by increased expression of renal 1α-hydroxylase gene. *Endocrinology* **143** 683-689.

Yoshiko Y, Candeliere GA, Maeda N & Aubin JE 2007a Osteoblast autonomous Pi regulation via Pit1 plays a role in bone mineralization. *Mol Cell Biol* **27** 4465-4474.

Yoshiko Y, Wang H, Minamizaki T, Ijuin C, Yamamoto R, Suemune S, Kozai K, Tanne K, Aubin JE & Maeda N 2007b Mineralized tissue cells are a principal source of FGF23. *Bone* **40** 1565-1573.

Figure legends

Figure 1 Recruitment of sKL increases ERK1/2 activation in parietal bones of *kl/kl* mice without changes in serum calcium and phosphate levels

Serum FGF23 (**A**), calcium (Ca) (**B**), phosphate (Pi) (**C**), and 1,25D (**C**) levels. FGF23 levels in bones and kidneys (**F**). mRNA levels of *Fgf23* in bones (**E**); *Cyp27b1* (**H**), *Slc34a1* (**I**), and *Slc34a3* (**J**) in kidneys; *Galnt3* (**K**), and *Furin* (**L**) in bones and kidneys. (**G**) ERK1/2 phosphorylation in bones and kidneys. The following panels in (**G**) provide representative blotting images for each group. pERK1/2, phosphorylated ERK1/2. Values in (**E**, **G**–**L**) are relative to the wild-type (WT), which is set at 1.0. Data represent mean ± SD. * $P < 0.05$ and ** $P < 0.01$, compared to WT mice. $n = 9$.

Figure 2 A single intravenous administration of sKL to normal mice pretreated with 1,25D increased ERK1/2 activation in parietal bones

Fgf23 mRNA levels in bones (**A**) and FGF23 levels in bones, kidneys (**B**), and sera (**C**). Serum calcium (Ca) (**D**) and phosphate (Pi) (**E**) levels. mRNA levels of *Slc34a1* (**F**), *Slc34a3* (**G**), and *Cyp27b1* (**H**) in kidneys. ERK1/2 phosphorylation in bones (**I**) and kidneys (**J**). pERK1/2, phosphorylated ERK1/2. Panels (**I, J**) are representative blotting images for each group. Values in (**A**, **F**–**J**) are relative to vehicle control is set at 1.0. Data represent mean ± SD. * $P < 0.05$ and ** $P < 0.01$, compared to vehicle control. $^{\#}$ $P < 0.05$, compared to 1,25D alone. $n = 6$. –, vehicle control; D, 1,25D alone; D+sKL, 1,25D plus sKL, respectively.

Figure 3 Recruitment of sKL caused hypomineralization in parietal bones of *kl/kl* mice

Representative images of frontal plastic (**A**, **B**) and decalcified paraffin (**C**) sections. (**A**) Elemental mapping of calcium (Ca), phosphorus (P), and magnesium (Mg). Right panel shows a color index for the level of each element. (**B**) Calcein-double labeling and calculated mineral apposition rate (MAR). (**C**) Hematoxylin and eosin staining. The parentheses in the figure indicate the osteoid. Scale bar, 5 μm (**B**) and 25 μm (**C**). Histomorphometry analysis of unmineralized osteoid thickness (OsTh) (**D**), number of osteoblasts per bone surface (NOb/BS) (**E**), osteocyte lacunae per bone area (NOc/BAR) (**F**), and bone thickness (BTh) (**G**). * P < 0.05 and * P < 0.01, compared to wild-type (WT) mice that received the vehicle. # $P < 0.05$, compared to *kl/kl* mice that received the vehicle. $n = 9$.

Figure 4 Recruitment of Klotho increased ERK activation in the parietal bones of *kl/kl* mice (**A**) Representative images of immunofluorescence staining of FGF23-positive osteoblasts/osteocytes costained with anti-phosphorylated ERK (pERK) antibodies. Decalcified paraffin sections of parietal bones were used, as shown in Figure 3C. Scar bars, 25 μm. (**B**–**J**) mRNA levels of osteoblast/osteocyte-associated genes. Values are relative to wild-type (WT) mice as controls that are set at 1.0. Data represent mean ± SD. * $P < 0.05$, compared to WT mice that received the vehicle. $n = 9$.

Figure 5 sKL contributed to FGF23 signaling in bones, resulting in decreased matrix mineralization

(**A**−**D**) Calvaria cell cultures of WT and *kl/kl* mice. Alkaline phosphatase-positive (ALP^+) area (**A**) and mineralization foci (**B**). (**C**) FGF23 levels in culture media of WT and *kl/kl* as indicated in time (day). Data represent mean ± SD. * $P < 0.05$ and ** $P < 0.01$, compared to

WT mice. *n* = 8−9. (**D**) mRNA expression of *Fgf23* and *Klotho* in bones and kidneys at day3 (d3) and day10 (d10). (**E-G**) Parietal bones from newborn WT or *kl/kl* mice. (**E**) Medium FGF23 concentrations, *Egr-1* mRNA levels (**F**), and ERK1/2 phosphorylation (**G**). Panels below (**G**) are representative blotting images for each group. Data represent mean ± SD. * $P < 0.05$ and ** $P < 0.01$, compared to matched vehicle control (−). *n* = 4. (**H-J**) Fetal rat calvaria cells. *Egr-1* mRNA levels (**H**) and ERK1/2 phosphorylation (**I**). Panels below are representative blotting images for each group. (**J**) Immunoblotting (IB) with polyclonal anti-FGF23 antibody (αFGF23) after immunoprecipitation (IP) with monoclonal anti-FGFR1 antibody (αFGFR1). Data represent mean ± SD. ** $P < 0.01$, compared to matched vehicle control (−). *n* = 4.

Figure 6 PHEX is a downstream target of sKL and FGF23 in the bones

(**A, E, F**) The number of mineralized foci in fetal rat calvarial (RC) cell cultures. X-axis values in (**A**), μg/ml. (**B-D**) *Phex* mRNA levels in RC cells. Values are relative to matched controls, which is set at 1.0. (**E**) sPHEX, soluble PHEX. (**F**) U, U0126 (U); Dic, dicumarol; and SB, SB203580. Data represent mean ± SD.* $P < 0.05$ and ** $P < 0.01$, compared to matched vehicle control (−); # $P < 0.05$, compared to sKL/FGF23. *n* = 4.

Figure 7 A schematic summary of the circulation and function of sKL and FGF23.

sKL, truncated from membrane Klotho in kidneys, circulates and acts in bones but not kidneys, by forming a complex with FGFR1 and FGF23, which is expressed in bone. This upregulates ERK1/2 signaling, resulting in downregulation of Phex in osteoblasts-osteocytes and resultant hypomineralization of bone.

Supplementary Figure 1 Serum FGF23 levels with body weight changes in WT vs *kl/kl* mice

(**A**) Serum FGF23 levels in WT and *kl/kl* mice at day 7, 21, 30, and 42. (**B**) Body weight changes in WT and *kl/kl* mice with and without sKL at day 10, 13, 16, 19, and 22. Data represent mean ± SD. * $P < 0.05$ and *** $P < 0.001$, compared to WT mice. $n = 9-10$.

Supplementary Figure 2 The RGB color intensity of electron probe X-ray microanalysis of parietal bones

Quantification of the RGB (red, green, and blue) color intensity of the representative image shown in **Figure 3A.** Values are relative to WT mouse bones, which is set at 1.0.

Figure 1

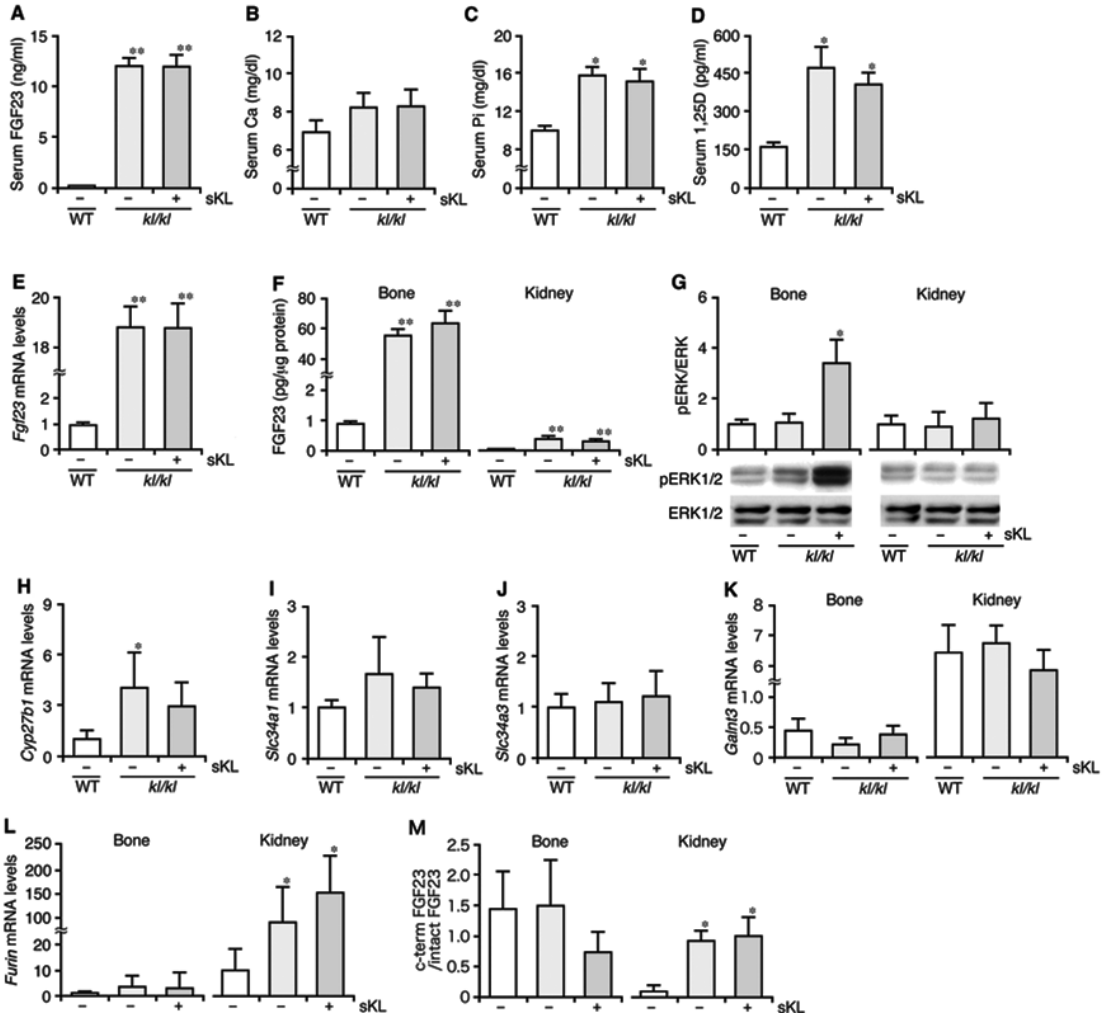
A
Serum FGF23 (ng/ml)
B
Serum Ca (mg/dl)
C
Serum Pi (mg/dl)
D
Serum 1,25D (pg/ml)
E
Fgf23 mRNA levels
F
FGF23 (pg/μg protein)
Bone
Kidney
G
pERK/ERK
pERK1/2
ERK1/2
H
Cyp27b1 mRNA levels
I
Slc34a1 mRNA levels
J
Slc34a3 mRNA levels
K
Galnt3 mRNA levels
L
Furin mRNA levels
M
c-term FGF23 /intact FGF23
WT
kl/kl
sKL

Figure 2

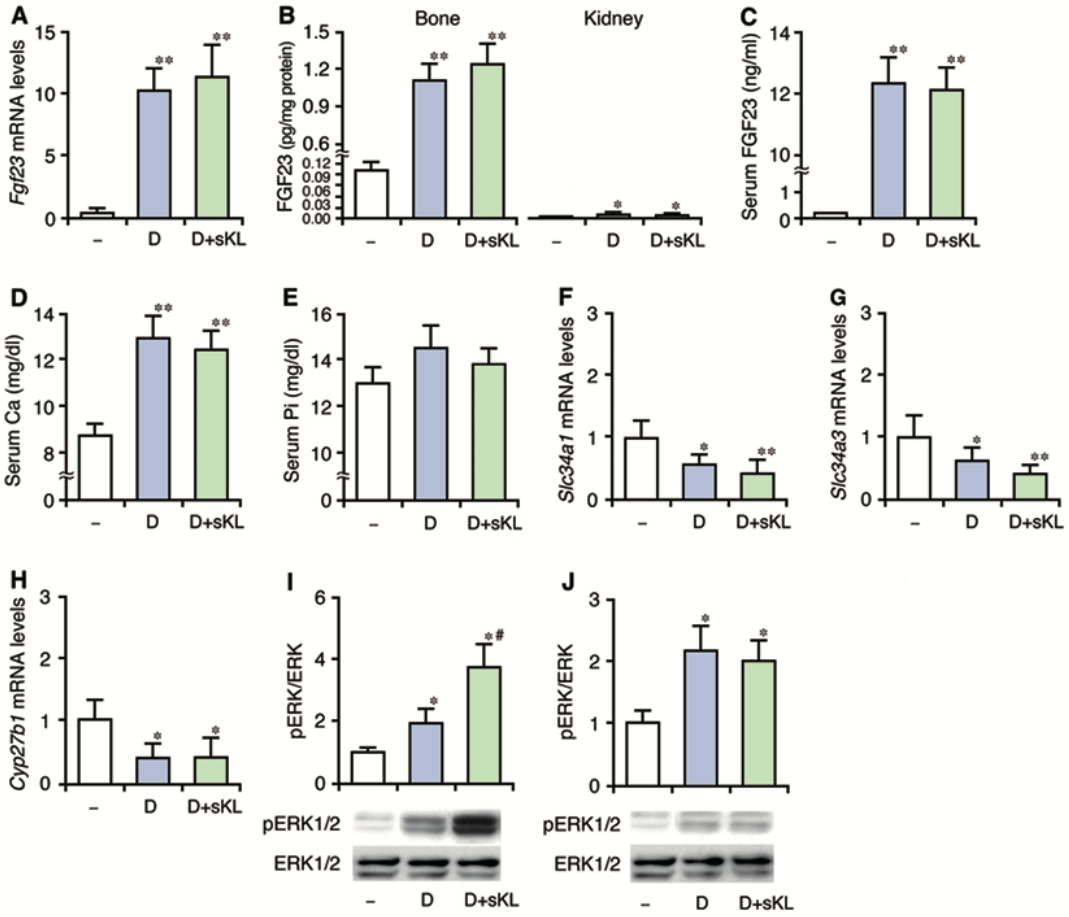
A
Fgf23 mRNA levels
B
Bone
Kidney
FGF23 (pg/mg protein)
C
Serum FGF23 (ng/ml)
D
Serum Ca (mg/dl)
E
Serum Pi (mg/dl)
F
Slc34a1 mRNA levels
G
Slc34a3 mRNA levels
H
Cyp27b1 mRNA levels
I
pERK/ERK
pERK1/2
ERK1/2
J
pERK/ERK
pERK1/2
ERK1/2
–
D
D+sKL

Figure 3

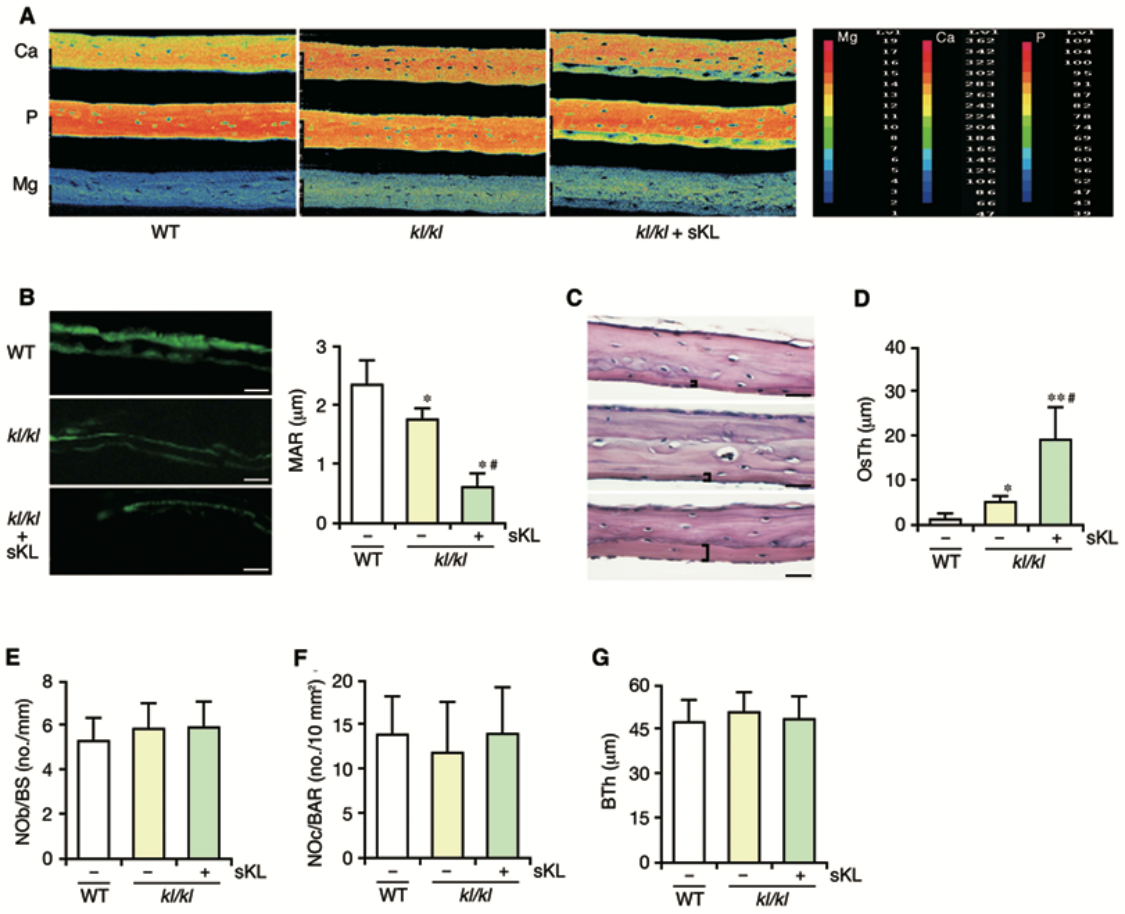
A
Ca
P
Mg
WT
kl/kl
kl/kl + sKL
B
WT
kl/kl
kl/kl + sKL
MAR (μm)
sKL
C
D
OsTh (μm)
E
NOb/BS (no./mm)
F
NOc/BAR (no./10 mm²)
G
BTh (μm)

Figure 4

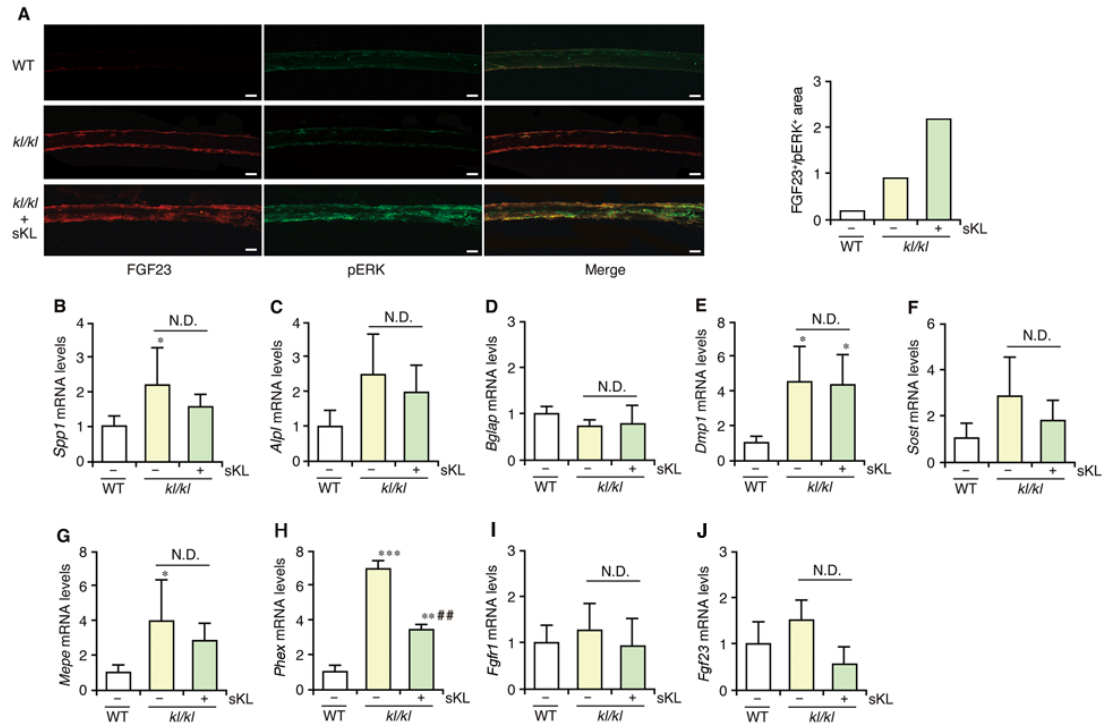
A
WT
kl/kl
kl/kl + sKL
FGF23
pERK
Merge
FGF23+/pERK+ area
sKL
WT
kl/kl
B
Spp1 mRNA levels
C
Alpl mRNA levels
D
Bglap mRNA levels
E
Dmp1 mRNA levels
F
Scst mRNA levels
G
Mepe mRNA levels
H
Phex mRNA levels
I
Fgfr1 mRNA levels
J
Fgf23 mRNA levels
N.D.

Figure 5

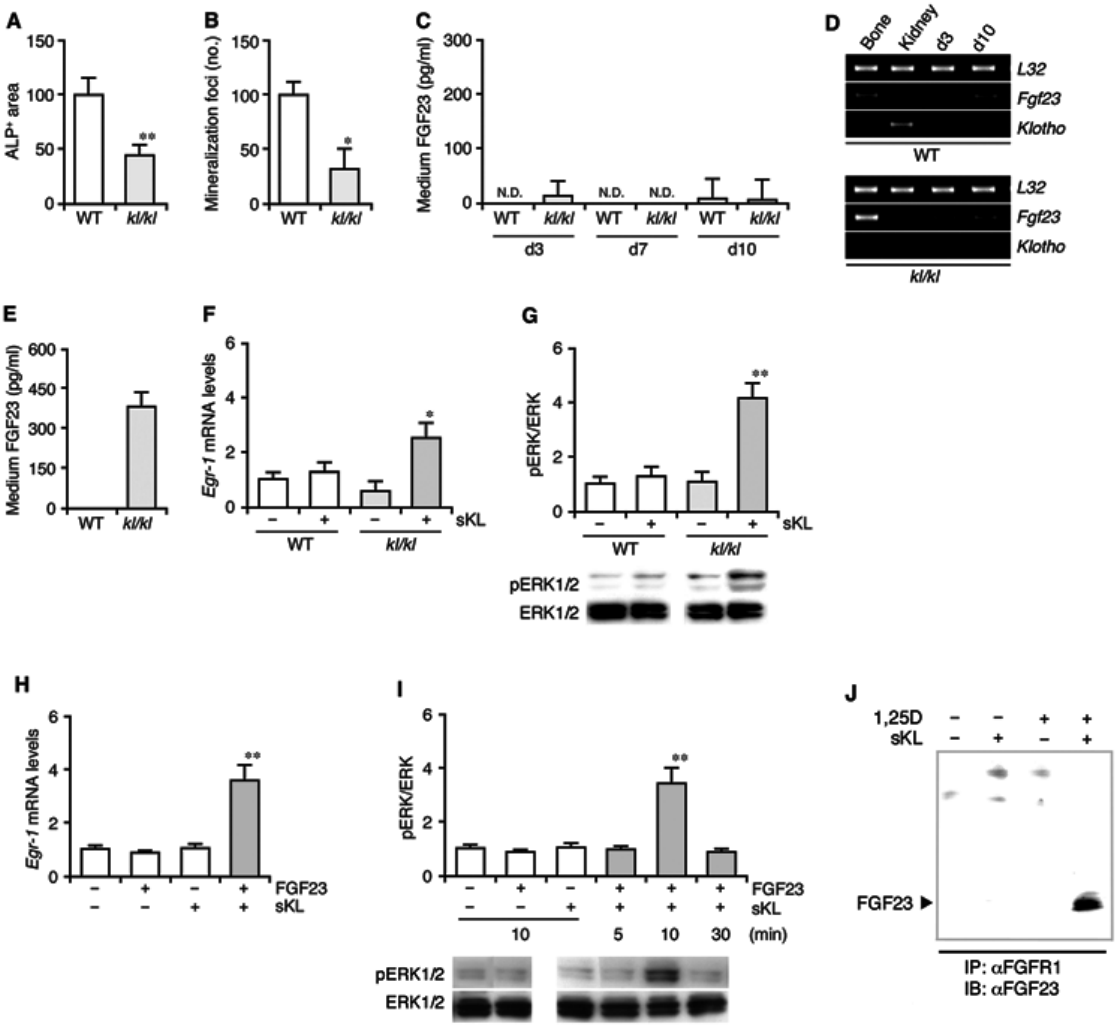
A
ALP+ area
150
100
50
0
WT
kl/kl
**
B
Mineralization foci (no.)
150
100
50
0
WT
kl/kl
*
C
Medium FGF23 (pg/ml)
300
200
100
0
N.D.
N.D.
N.D.
WT
kl/kl
WT
kl/kl
WT
kl/kl
d3
d7
d10
D
Bone
Kidney
d3
d10
L32
Fgf23
Klotho
WT
L32
Fgf23
Klotho
kl/kl
E
Medium FGF23 (pg/ml)
600
450
300
150
0
WT
kl/kl
F
Egr-1 mRNA levels
6
4
2
0
*
– + – +
sKL
WT
kl/kl
G
pERK/ERK
6
4
2
0
**
– + – +
sKL
WT
kl/kl
pERK1/2
ERK1/2
H
Egr-1 mRNA levels
6
4
2
0
**
– + – +
– – + +
FGF23
sKL
I
pERK/ERK
6
4
2
0
**
– + – + + +
– – + + + +
FGF23
sKL
10
5
10
30
(min)
pERK1/2
ERK1/2
J
1,25D – – + +
sKL – + – +
FGF23
IP: αFGFR1
IB: αFGF23

Figure 6

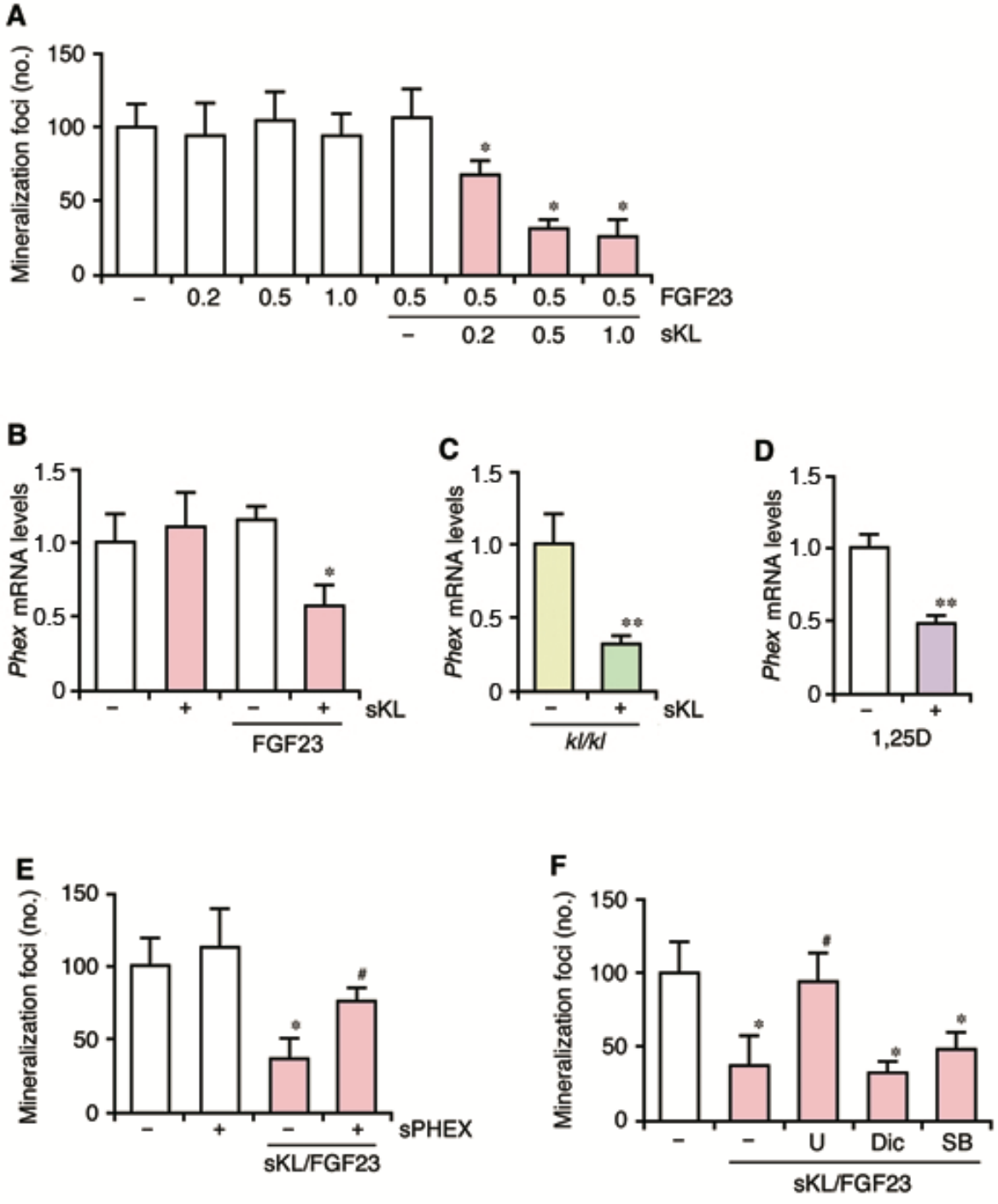
A
Mineralization foci (no.)
150
100
50
0
–
0.2
0.5
1.0
0.5
0.5
0.5
0.5
FGF23
–
0.2
0.5
1.0
sKL
B
Phex mRNA levels
1.5
1.0
0.5
0
–
+
–
+
sKL
FGF23
C
Phex mRNA levels
1.5
1.0
0.5
0
–
+
sKL
kl/kl
D
Phex mRNA levels
1.5
1.0
0.5
0
–
+
1,25D
E
Mineralization foci (no.)
150
100
50
0
–
+
–
+
sPHEX
sKL/FGF23
F
Mineralization foci (no.)
150
100
50
0
–
–
U
Dic
SB
sKL/FGF23

Figure 7

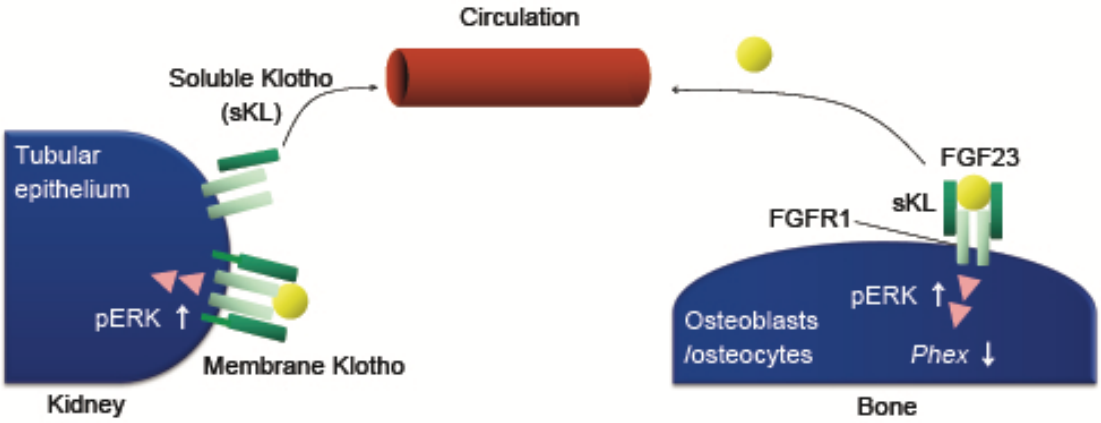
Circulation
Soluble Klotho
(sKL)
Tubular
epithelium
pERK
Membrane Klotho
Kidney
FGF23
sKL
FGFR1
pERK
Osteoblasts
/osteocytes
Phex
Bone

Supplementary Figure 1

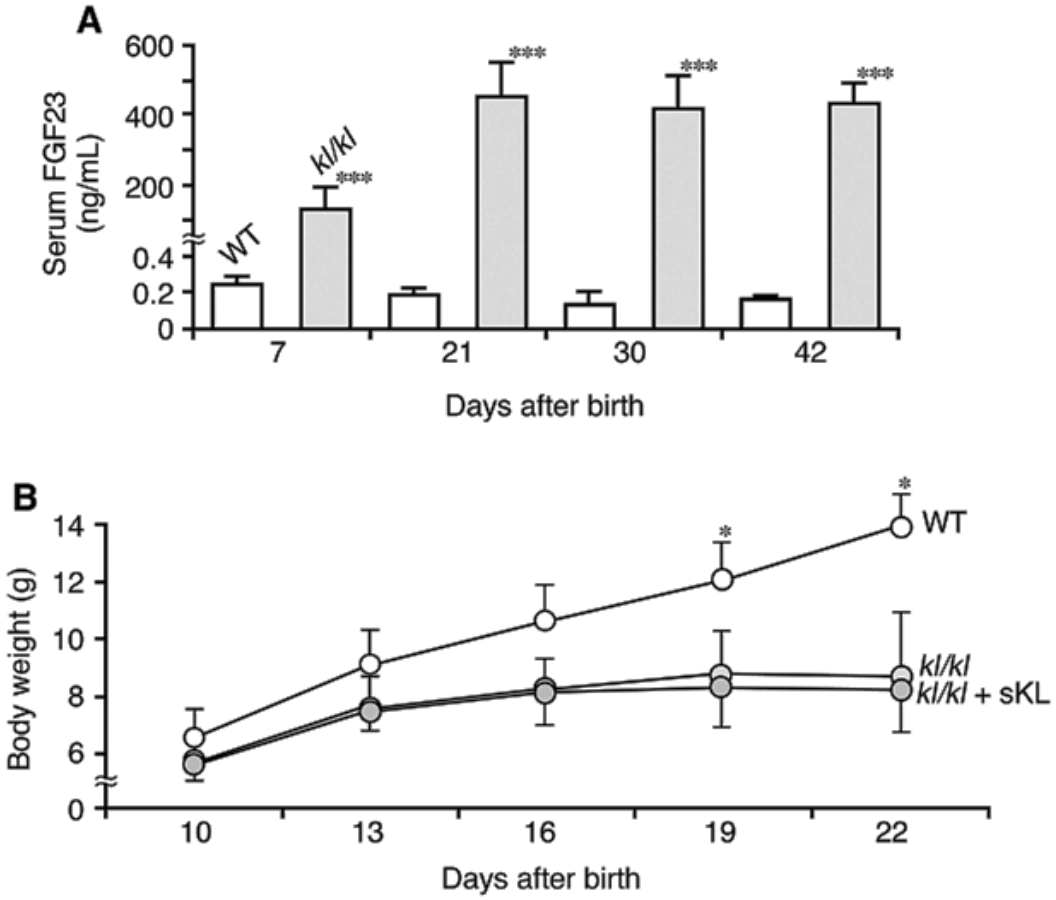

Supplementary Figure 2

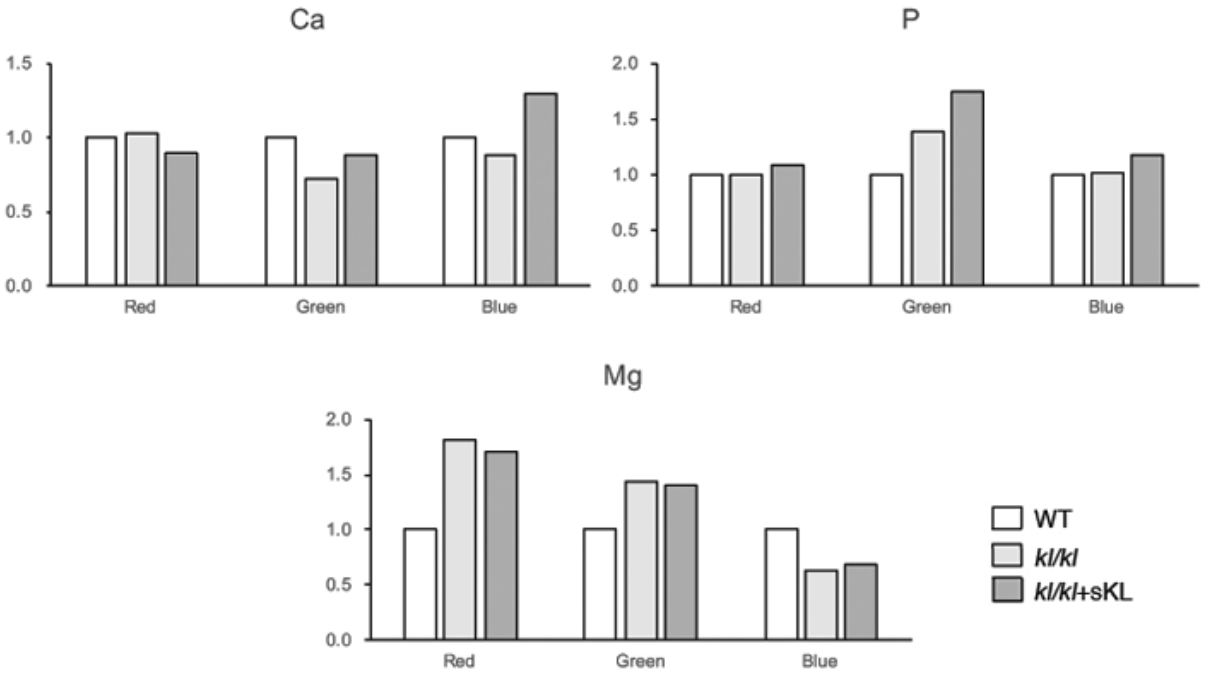

Supplementary Table 1				
Species	Target		Sequence	Size
Rat	*Alp*	F	CTG CAA GGA CAT CGC CTA TC	101
		R	CAT CAG TTC TGT TCT TGG GGT A	
	Egr-1	F	CCT ATG AGC ACC TGA CCA CA	196
		R	AGG CCA CTG ACT AGG CTG AA	
	Fgf23	F	TAA TAG GGG CCA TGA CCA GA	145
		R	TGA TGC TTC GGT GAC AGG TA	
	Klotho	F	GGGACCACCAGAAGAGATGA	437
		R	TTGGCTACAACCCCGTCTAC	
	Phex	F	CCT CCT ACC AGG CAT CAC AT	126
		R	GGA GGA CTG TGA GCA CCA AT	
	Rpl32	F	GAT TCA AGG GCC AGA TCC T	66
		R	GCA TGT GCT TGG TTT TCT TG	
Mouse	*Actb*	F	TTT TCC AGC CTT CCT TCT TG	89
		R	ACG GAT GTC AAC GTC ACA CT	
	Alp	F	TGG CCT GGA TCT CAT CAG TA	75
		R	GTG CGG TTC CAG ACA TAG TG	
	Bglap	F	AAG CAG GAG GGC AAT AAG GT	274
		R	ACT TGC AGG GCA GAG AGA GA	
	Cyp27b1	F	CAG CTT CCT GGC TGA ACT CT	93
		R	GAC CAT ATT GGC CCG TAC C	
	Dmp1	F	CCC ACG AAC AGT GAG TCA TC	75
		R	GCT GTC CGT GTG GTC ACT AT	
	Fgf2	F	CAA CCG GTA CCT TGC TAT GA	119
		R	TCC GTG ACC GGT AAG TAT TG	
	Fgf23	F	TTT GGA TCG CTT CAC TTC AGC	101
		R	ACC AGG TAG TGA TGC TTC TGC	
	Fgfr1	F	TTT AAG CCT GAC CAC CGA AT	83
		R	TCA GAA GGC ACC ACA GAA TC	
	Furin	F	CCA CCA AGC CCT TTC TAA CA	90
		R	TGC AAA AGG CAC ATC AGA AG	
	GaInt3	F	GGA GGC AAA CCA TTG ATT CT	74
		R	CGC TGA GCA GAA TAC TCG AA	
	Klotho	F	CAA AAG GGA TGA TGC CAA AT	144
		R	CTG TAG CCC CTA TGC CAC TC	
	Mepe	F	CTC ATG AAG ATG CAG GCT GT	89
		R	CAG CTG CTC CTG TCT TCA TT	
	Opn	F	CCA TGA GAT TGG CAG TGA TT	89
		R	CTC CTC TGA GCT GCC AGA AT	
	Phex	F	ATT GCA CTG GCC CTG TTT AT	86
		R	GCT TGG AAA CTT AGG AGA CCT T	
	Rpl32	F	AGT TCA TCA GGC ACC AGT CA	72
		R	TGT CAA TGC CTC TGG GTT T	
	Slc34a1	F	CTC ATT GTG GGT GCC CAA CAT GAT G	90
		R	ACC ATG TGT CTC CCA CGG ACT GGA AG	
	Slc34a3	F	CCA GCT GGA TAG CAG TGT GA	173
		R	TGT CCT CCT CTG GAG ATG CT	
	Sost	F	AAG GGA GTG TGG AAC GAA AG	112
		R	GGT CAG GGT CAG AAA CCC TA	

Supplementary Table 2

Upregulated				Downregulated			
Gene	Intensity		Fold change	Gene	Intensity		Fold change (log)
	β-gal	FGF23			β-gal	FGF23	
RT1-EC2	18.3	50.2	1.7	*Rdx*	250.8	97.1	-1.3
Transcribed locus	59.7	167.2	1.4	*Phex*	133.9	68.3	-1.2
Transcribed locus	384.5	997.7	1.4	Transcribed locus	251.3	105.7	-1.2
Egln3	13.1	31.9	1.4	*Zfp422*	108.6	58.9	-1.2
Slx1b	55.3	153.9	1.3	Transcribed locus	38.3	17	-1.2
S100a13	53.6	154.3	1.3	*Fgl2*	34.5	12.7	-1.2
RT1-EC2	10.1	24.9	1.3	Transcribed locus	205.8	96.7	-1.2
Gnb1	99.4	271	1.3	*Ythdf2*	628.7	247.1	-1.1
Cdkn1a	238.1	500.6	1.3	Transcribed locus	91.6	43.8	-1.1
Transcribed locus	204.4	456.9	1.2	*Dusp6*	111.5	48.5	-1.1
Transcribed locus	63.6	190.3	1.2	Transcribed locus	145.5	62.4	-1.1
Mnf1	269.3	624.4	1.2	Transcribed locus	65.6	33	-1.1
Cklf	22.8	54.4	1.2	*Lin7c*	232.2	120.4	-1
Atox1	185.5	425.3	1.2	Transcribed locus	749	386.2	-1
(miscRNA)	64.6	131.5	1.2	Transcribed locus	67.1	44.1	-1
Ubl7	63.4	124.9	1.1	Transcribed locus	76.4	37.9	-1
RGD1565641	265.8	663.2	1.1				
Lcp1	11.7	28.6	1.1				
Emg1	74.4	144	1.1				
Usmg5	931.1	1821.5	1				
Transcribed locus	33.6	67.9	1				
TL0ABA24YI10	436.4	775.6	1				
Slirp	200.6	410.5	1				
Rps25	1364.4	2846.6	1				
RGD1309621	555.2	1161	1				
RGD1309621	259.3	447.6	1				
Polr2l	337.7	538.4	1				
Polr2i	245.5	489.6	1				
Nop10	772.2	1506.6	1				
Ndufa11	407.7	844.9	1				
Mrpl14	29.1	50.5	1				
Eif3k	604.9	1283.7	1				
Csde1	440	871.6	1				
Churc1	432.1	909.2	1				
Atp5j2	632.8	1253.6	1				